http://www.aimspress.com/journal/mine

Mathematics in Engineering, 1(3): 419–433.
DOI:10.3934/mine.2019.3.419
Received: 14 December 2018
Accepted: 25 February 2019
Published: 30 April 2019

Research article

Metastability of solitary waves in diatomic FPUT lattices†

Nickolas Giardetti, Amy Shapiro, Stephen Windle and J. Douglas Wright*

Department of Mathematics, Drexel University, 3141 Chestnut St, Philadelphia, PA 19104

† **This contribution is part of the Special Issue:** Hamiltonian Lattice Dynamics
Guest Editors: Simone Paleari; Tiziano Penati
Link: http://www.aimspress.com/newsinfo/1165.html

* **Correspondence:** Email: jdw66@drexel.edu.

Abstract: It is known that long waves in spatially periodic polymer Fermi-Pasta-Ulam-Tsingou lattices are well-approximated for long, but not infinite, times by suitably scaled solutions of Korteweg-de Vries equations. It is also known that dimer FPUT lattices possess nanopteron solutions, *i.e.,* traveling wave solutions which are the superposition of a KdV-like solitary wave and a very small amplitude ripple. Such solutions have infinite mechanical energy. In this article we investigate numerically what happens over very long time scales (longer than the time of validity for the KdV approximation) to solutions of diatomic FPUT which are initially suitably scaled (finite energy) KdV solitary waves. That is we omit the ripple. What we find is that the solitary wave continuously leaves behind a very small amplitude "oscillatory wake." This periodic tail saps energy from the solitary wave at a very slow (numerically sub-exponential) rate. We take this as evidence that the diatomic FPUT "solitary wave" is in fact quasi-stationary or metastable.

Keywords: diatomic Fermi-Pasta-Ulam-Tsingou lattices; metastability; Hamiltonian lattices; solitary waves; nonlinear waves

1. Introduction

We consider a diatomic Fermi-Pasta-Ulam-Tsingou (FPUT) lattice as depicted in Figure 1 below. Newton's second law gives the equations of motion:

$$m_n \ddot{x}_n = F(x_{n+1} - x_n) - F(x_n - x_{n-1}).$$

To be clear, here $x_n(t)$ is the position of the nth (with $n \in \mathbf{Z}$) particle at time t. We assume that the masses satisfy

$$m_{n+2} = m_n \text{ for all } n \in \mathbf{Z}$$

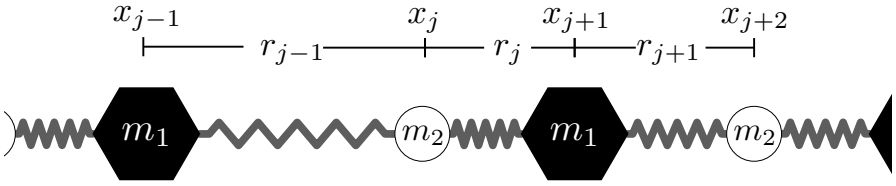

Figure 1. A segment of an FPUT lattice. The mass of the nth particle is m_n and its position is x_n. The springs exerts a force $F(r)$, which is a function of the relative displacement $r_n := x_{n+1} - x_n$. The motion is constrained to be in the line. In this figure, j is even.

and the spring force is

$$F(r) := r + r^2.$$

That is to say the lattice is a so-called "mass dimer," as studied in [1–12]. It is convenient and technically advantageous to rewrite the system in terms of the relative displacements $r_n := x_{n+1} - x_n$ and velocities $p_n := \dot{x}_n$:

$$\dot{r}_n = p_{n+1} - p_n \quad \text{and} \quad \dot{p}_n = \frac{1}{m_n}\left(F(r_n) - F(r_{n-1})\right). \tag{1.1}$$

We are principally interested in the long time dynamics of finite energy* solutions $\mathbf{r}(t) := (r(t), p(t))$ which are of long wavelength and small amplitude. This situation is sometimes called "the KdV limit" for, as shown in [4, 7, 13], such solutions of (1.1) are well-approximated for long, but finite, times by suitably scaled solutions of Korteweg-de Vries equations. KdV equations famously possess solitary wave solutions and as such the approximation results indicate that (1.1) has a solution which is "solitary wave-like," at least for very long times. In particular, for $0 < \varepsilon \ll 1$, there is a solution of (1.1) of the form

$$\mathbf{r}_n(t) = \mathbf{\Psi}_n^{m_1,m_2,\varepsilon}(t) := 3\varepsilon^2 \operatorname{sech}^2\left(\beta\varepsilon\,(n - c_\varepsilon t)\right)\mathbf{v} + \mathbf{z}_n(t)$$

where

$$\beta := \sqrt{\frac{3(m_1^2 + 2m_1m_2 + m_2^2)}{2(m_1^2 - m_1m_2 + m_2^2)}}, \quad c_\varepsilon := (1+\varepsilon^2)\sqrt{\frac{2}{m_1+m_2}} \quad \text{and} \quad \mathbf{v} := (1, -c_0). \tag{1.2}$$

The quantity c_ε is the wave-speed and c_0 is called "the speed of sound." The error† function $\mathbf{z}(t)$ is less than $O_{\ell^2\times\ell^2}(\varepsilon^{5/2})$ for $|t| \le T_0/\varepsilon^3$. In this article we take $\mathbf{z}(0) = 0$, though the results in [4, 7] allow a fair bit of latitude for its initial value. The key question of this article is this: *What happens to $\mathbf{\Psi}^{m_1,m_2,\varepsilon}(t)$ for times much greater than $O(1/\varepsilon^3)$?* In the monatomic problem, *i.e.,* when $m_1 = m_2 = m > 0$, the system (1.1) possesses a family of supersonic (that is, with speeds $c > c_0$) solitary wave solutions which are asymptotically stable with respect to perturbations initially small in $\ell^2 \times \ell^2$ ([14–18]). This solitary wave is given by

$$\mathbf{r}_n(t) = \mathbf{\Sigma}_n^{m,\varepsilon}(t) := 3\varepsilon^2 \operatorname{sech}^2\left(\beta\varepsilon(n - c_\varepsilon t)\right)\mathbf{v} + \boldsymbol{\eta}_\varepsilon(n - c_\varepsilon t).$$

*Naturally the system conserves energy. Specifically $E(t) := \sum_{n\in\mathbf{Z}}\left(\frac{1}{2}m_n p_n^2(t) + \frac{1}{2}r_n^2(t) + \frac{1}{3}r_n^3(t)\right)$ is constant so long as it is initially finite. It is straightforward to show that, so long as $\|r\|_{\ell^2}$ is not too big, $\sqrt{E}$ is equivalent to $\|(r,p)\|_{\ell^2\times\ell^2}$.

†If $m_1 = m_2$ the error estimate is stronger: $\mathbf{z}(t)$ is $O_{\ell^2\times\ell^2}(\varepsilon^{7/2})$.

The constants β, c_ε and $\mathbf{v}$ are exactly as in (1.2). The function $\boldsymbol{\eta}_\varepsilon(y)$ is small and spatially localized in the sense that there exists $\widetilde{\beta} > 0$ such that $\cosh(\widetilde{\beta}y)\boldsymbol{\eta}_\varepsilon(y/\varepsilon) = O_{H^s\times H^s}(\varepsilon^4)$. As such we can divine the ultimate fate of the solution $\boldsymbol{\Psi}^{m,m,\varepsilon}(t)$ in the monatomic case:

$$\boldsymbol{\Psi}^{m,m,\varepsilon}(t) \longrightarrow \boldsymbol{\Sigma}_n^{m,\varepsilon'}(t-t') \quad \text{as} \quad t \longrightarrow \infty$$

for some $\varepsilon' \sim \varepsilon$ and $t' \sim 0$. Note that the convergence is not in $\ell^2 \times \ell^2$, but in a somewhat more complicated space. See [18] for the details.

On the other hand, the recent work in [1, 2, 11, 12] demonstrates that for a mass dimer the natural analog of the monatomic solitary wave is a "generalized solitary wave", *i.e.,* a traveling wave which is the superposition of a core which is qualitatively a solitary wave and a very small amplitude periodic "ripple." Such solutions are sometimes called "nanopterons" [19]. Specifically, when $m_1 \neq m_2$ and $\varepsilon > 0$ is not too large, there is a solution of (1.1) of the form

$$\mathbf{r}_n(t) = \boldsymbol{\Gamma}_n^{m_1,m_2,\varepsilon}(t) := \underbrace{3\varepsilon^2 \operatorname{sech}^2(\beta\varepsilon(n-c_\varepsilon t))\,\mathbf{v} + \boldsymbol{\eta}_{n,\varepsilon}(n-c_\varepsilon t)}_{\text{the solitary core}} + \underbrace{\boldsymbol{\phi}_{n,\varepsilon}(n-c_\varepsilon t)}_{\text{the ripple}}.$$

In the above, β, c_ε and $\mathbf{v}$ are as in (1.2). The functions $\boldsymbol{\eta}_{n,\varepsilon}(y)$ and $\boldsymbol{\phi}_{n,\varepsilon}(y)$ satisfy:

$$\boldsymbol{\eta}_{n+2,\varepsilon}(y) = \boldsymbol{\eta}_{n,\varepsilon}(y) \text{ and } \boldsymbol{\phi}_{n+2,\varepsilon}(y) = \boldsymbol{\phi}_{n,\varepsilon}(y) \text{ for all } n \in \mathbf{Z} \text{ and } y \in \mathbf{R}.$$

Which is to say that, with respect to the subscript n, they have the same periodicity as the lattice. Moreover there exists a constant $\widetilde{\beta} > 0$ such that $\cosh(\widetilde{\beta}y)\boldsymbol{\eta}_{n,\varepsilon}(y/\varepsilon) = O_{H^s\times H^s}(\varepsilon^3)$, *i.e.,* the $\boldsymbol{\eta}_{n,\varepsilon}$ are small and go to zero exponentially fast at spatial infinity. The functions $\boldsymbol{\phi}_{n,\varepsilon}(y)$ are spatially periodic. Their frequency is $\xi_\varepsilon = \xi_0 + O(\varepsilon)$ where $\xi_0 = \xi_0(m_1, m_2)$ is the unique positive solution of the "phase resonance" condition

$$c_0^2\xi_0^2 = \frac{1}{m_1} + \frac{1}{m_2} + \sqrt{\left(\frac{1}{m_1} - \frac{1}{m_2}\right)^2 + \frac{4\cos^2(\xi_0)}{m_1 m_2}}. \tag{1.3}$$

The amplitudes of $\boldsymbol{\phi}_{n,\varepsilon}(y)$ are small beyond all orders of ε; for all $n \in \mathbf{N}$,

$$\lim_{\varepsilon\to 0^+} \varepsilon^{-n}\|\boldsymbol{\phi}_{n,\varepsilon}\|_{W^{s,\infty}\times W^{s,\infty}} = 0.$$

Without being too technical, in the diatomic problem the dispersion relation for (1.1) has two branches whereas the monatomic problem has a single branch. The first of the diatomic problem's branches is called the "acoustic branch" and it is qualitatively similar to the dispersion relation for the monatomic problem. Roughly speaking, the acoustic part of the diatomic problem can, in isolation, support a solitary wave at speeds slightly above the speed of sound c_0. The second branch is called the "optical branch." As it happens, this branch has plane wave solutions which can propagate with any phase speed. As such, the nonlinearity in the problem causes the acoustic branch solitary wave to resonate weakly with plane waves with the speed of sound, ultimately generating the ripple. The spatial frequency at which this resonance occurs is ξ_0 in (1.3). See [1, 11, 20] for a more in depth treatment.

Despite the fact that it is so small, the presence of the ripple precludes membership of $\mathbf{\Gamma}^{m_1,m_2,\varepsilon}$ in $\ell^2 \times \ell^2$, since this solution does not converge[‡] to zero as $|j| \to \infty$. Thus the generalized solitary wave has *infinite energy* and as such it is categorically impossible for the finite energy solution $\mathbf{\Psi}^{m_1,m_2,\varepsilon}(t)$ to converge to $\mathbf{\Gamma}^{m_1,m_2,\varepsilon}$ as $t \to \infty$. And so something else must happen, something which is quite different than the convergence to the solitary wave which takes place in the monatomic problem.

We study this by carefully simulating the solitary wave-like solution $\mathbf{\Psi}^{m_1,m_2,\varepsilon}(t)$ over very long times. The results are unambiguous: as $\mathbf{\Psi}^{m_1,m_2,\varepsilon}(t)$ propagates, it leaves behind a small amplitude, relatively high frequency "oscillatory wake." Initially somewhat disordered in appearance, the wake eventually settles into a rather regular periodic structure. Figure 2 contains a visualization of the simulations.

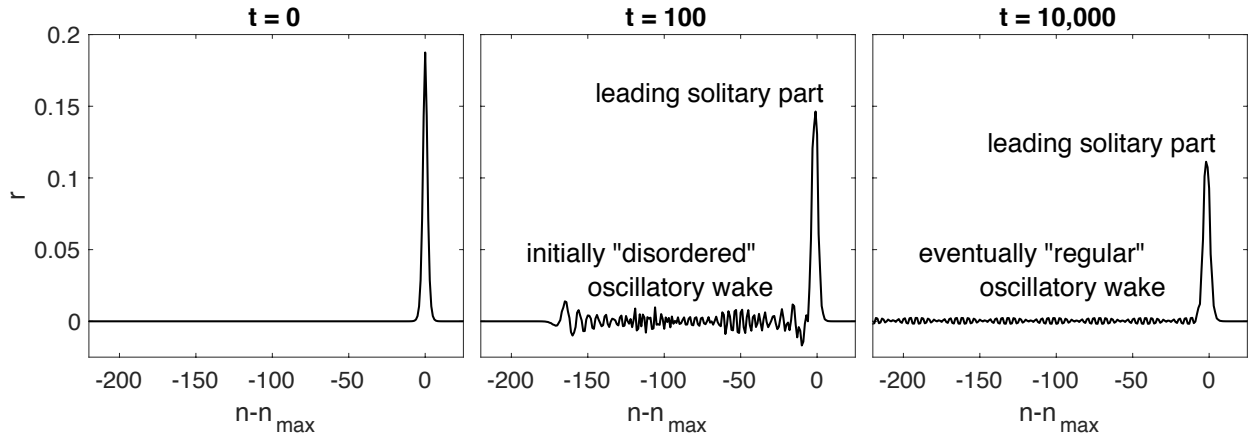

Figure 2. *Plots of the r−component of the numerical computation of* $\mathbf{\Psi}^{m_1,m_2,\varepsilon}(t)$ *vs. n at* $t = 100$ *and* $t = 10,000$. *In this figure,* $m_1 = 1$, $m_2 = 2$ *and* $\varepsilon = 1/4$. *The vertical scaling is the same in the three plots.*

While it is not atypical for small perturbations of solitary waves in nonlinear dispersive systems such as KdV or monatomic FPUT to leave a "dispersive tail" behind early on in their evolution, in those cases the tail "disconnects" from the main solitary wave and eventually falls far behind it. But in these diatomic FPUT problems, the oscillatory wake is generated during the entirety of the simulation, always immediately trailing the leading solitary wave and inexorably increasing in width.

The oscillatory wake was not unexpected—simulations for the "small mass ratio problem" (that is, $\varepsilon > 0$ is fixed and m_1/m_2 is taken to be very small) in [10] and [9] exhibit similar behavior. Those results were somewhat hobbled by the lack of computing power available at the time of their execution and as such the time scales of their runs were rather short. Also worth pointing out are the simulations of waves through lattices whose material properties randomly vary (as opposed to periodically vary) with respect to n. In this situation a "superdiffusive" effect is observed wherein the leading part of the pulse deteriorates very rapidly into "noise" [23], an effect similar too, but rather more pronounced, than what we see here.

[‡]It is worth pointing out that the results in [1, 11] do not prove that the amplitude of the ripple is nonzero and thus one might wonder if the ripple is really there or if its presence is a technical crutch. While there is some compelling formal evidence that for special values of m_1, m_2 and ε the ripple may in fact vanish [2, 12], our expectation is that in all but a set of measure zero in parameter space the ripple is nonzero. After all, this is the case for generalized solitary waves in the gravity-capillary problem [21, 22], a problem which, at a technical level, is rather similar to the FPUT problem considered here.

Our simulations run for times substantially longer than $1/\varepsilon^3$. An interesting finding: The frequency of the wake is largely independent of the leading wave's size and is not particularly close to the frequency ξ_ε of the ripple in the associated nanopteron. Moreover, as the width of the wake grows it slowly saps energy from the leading wave. In this way, the amplitude of the leading solitary wave slowly erodes during the evolution. The numerics indicate that the rate of this erosion is at most algebraic in t, much slower than the exponential rate one would expect were there a genuine linear instability. For these reasons, the solution $\mathbf{\Psi}^{m_1,m_2,\varepsilon}(t)$ is viewed as a *metastable* solitary wave.

2. The numerical method

Our numerical method for computing $\mathbf{\Psi}^{m_1,m_2,\varepsilon}(t)$, implemented in MATLAB, is rather straightforward. First we restrict the size of the domain to be $N = 2^{10}$. Specifically we take $n \in [-N/2+1, N/2] \cap \mathbf{Z}$ and enforce periodic boundary conditions in (1.1), that is $\mathbf{r}_{N/2}(t) = \mathbf{r}_{-N/2+1}(t)$ for all t. In this way we have converted the original infinite-dimensional system into a large finite-dimensional first-order system of differential equations. After picking m_1, m_2 and ε, we take the initial condition to be $\mathbf{r}_n(0) = 3\varepsilon^2 \operatorname{sech}^2(\beta\varepsilon j)\,\mathbf{v}$ with β and $\mathbf{v}$ as in (1.2). Then we simulate this system with a standard RK4 method. The time step is fixed at $h = 1/10$.

Because our simulations are to run for long periods and the oscillatory wake is relatively motionless in comparison to the leading solitary wave, we enforce a "windowing" on the numerically computed solution, lest the solitary wave interact with its wake after wrapping around the periodic box[§]. Specifically, at each time step t_l we compute the location n_{max} of the maximum of $\sqrt{r_n^2(t_l) + p_n^2(t_l)}$; this gives us the position of the leading solitary wave. Then we multiply $\mathbf{r}_n(t_l)$ by the function $W(j - n_{max} + N/8)$ where W is the N-periodic function which, for $k \in [-N/2+1, N/2]$, is given by:

$$W(k) := \begin{cases} 1 & \text{when } |k| \le \dfrac{5N}{16} \\ 1 - \dfrac{8}{N}\left(|k| - \dfrac{5N}{16}\right) & \text{when } \dfrac{5N}{16} < |k| \le \dfrac{7N}{16} \\ 0 & \text{when } \dfrac{7N}{16} < |k| \le \dfrac{N}{2}. \end{cases}$$

Consequently our numerical method will not come close to conserving energy: Energy leaves the leading solitary wave, goes into the wake and is eventually "zeroed out" by the window[¶]. Note, however, that our simulations indicate that anything that falls behind the solitary pulse has no further discernible effect on it (this is consistent with aspects of the stability theory for the monatomic solitary wave, which is known to "outrun" all disturbances [14–17]). Moreover, the size of the window is sufficiently large that the oscillatory wake is given enough time to settle down into a regular and consistent configuration. In this way, we are able to run our simulations for very long times in a way which focuses on the leading solitary wave and a very large part of the oscillatory

[§]Another way to avoid this problem would be to make the domain extremely large, on the order of $N = 10^7$. Such a remedy is obviously computationally expensive and hence we took another route

[¶]That the method as described will not conserve energy is one reason why we use an RK4 time stepping method, as opposed to, say, a more complicated symplectic structure preserving method (as in [24]).

wake. Since our main interest is on the formation of the wake immediately behind the solitary wave, the windowing is large enough to adequately resolve this phenomenon[‖].

3. Results

With our numerical method, we performed the following runs:

- Fixed $m_1 = 1$, $m_2 = \sqrt{2}$ and took $\varepsilon = 1/2, 1/4, 1/8, 1/16$.
- Fixed $m_1 = 1$, $m_2 = 2$ and took $\varepsilon = 1/2, 1/4, 1/8, 1/16$.
- Fixed $m_1 = 1$, $m_2 = \pi$ and took $\varepsilon = 1/2, 1/4, 1/8, 1/16$.

We picked these choices of masses so that we would have a mix of rational/irrational mass ratios as well as mass ratios which were large, small and close to one. Each run ran from $t = 0$ to $t = 10^6$. For each run, at each time step t_l we compute the amplitude of the main pulse:

$$amp_{sol}(t_l) := \max_n \sqrt{r_n^2(t_l) + p_n^2(t_l)} = \sqrt{r_{n_{max}}^2(t_l) + p_{n_{max}}^2(t_l)}.$$

Then we compute the amplitude of the solution at a fixed distance behind the location of the main pulse. This quantity gives us the size of the wake right after its formation. Specifically we use a "peak to trough" measure of the amplitude:

$$amp_{wake}(t_l) := \frac{1}{2}\left(\max_{n-n_{max}\in[-3N/4,-7N/8]} r_n(t_l) - \min_{n-n_{max}\in[-3N/4,-7N/8]} r_n(t_l)\right).$$

3.1. Profile snapshots

In Figures 3–5 we present snapshots of the of $r-$component of the numerical computation of $\mathbf{\Psi}^{m_1,m_2,\varepsilon}(t)$ vs. n at $t = 0$ and $t = 10^6$. That is, at the beginning and end of the run. Since the runs are so long, by the end of the run the amplitude of the oscillatory wake is quite small indeed and as such we provide "zooms" of these. Here are our observations:

1. The attenuation of the amp_{sol} is quite pronounced when ε is large, but when ε is small is barely discernible.
2. It is visible in these figures that, for fixed mass ratio, the spatial frequency of the wake is more or less constant across all simulated values of ε. The only variation from this is in in Figure 3 where the frequency when $\varepsilon = 1/16$ is notably different than for the other values of ε. We do not present this, but numerical computation of the frequency of the wake is all but constant (for fixed mass ratio and ε) in time once the disordered transient period has elapsed and the solution settles into the regular "wake plus solitary wave" form.
3. Note that in Figures 4 and 5 the wake at $\varepsilon = 1/16$ oscillates about a non-zero value. Note also that the amplitude of the wake in these cases is extremely small: $O(10^{-9})$ and $O(10^{-10})$, respectively. In these cases we are at the limit of the precise quantitative accuracy of our method. We include these principally because the qualitative dynamics are in line with the other simulations.

[‖]An interesting project would be to carry out the rigorous numerical analysis of this method. As pointed out by one of the referees, the method as described has features in common with the "freezing" method in [25,26] and as such those articles point towards a strategy for such an analysis.

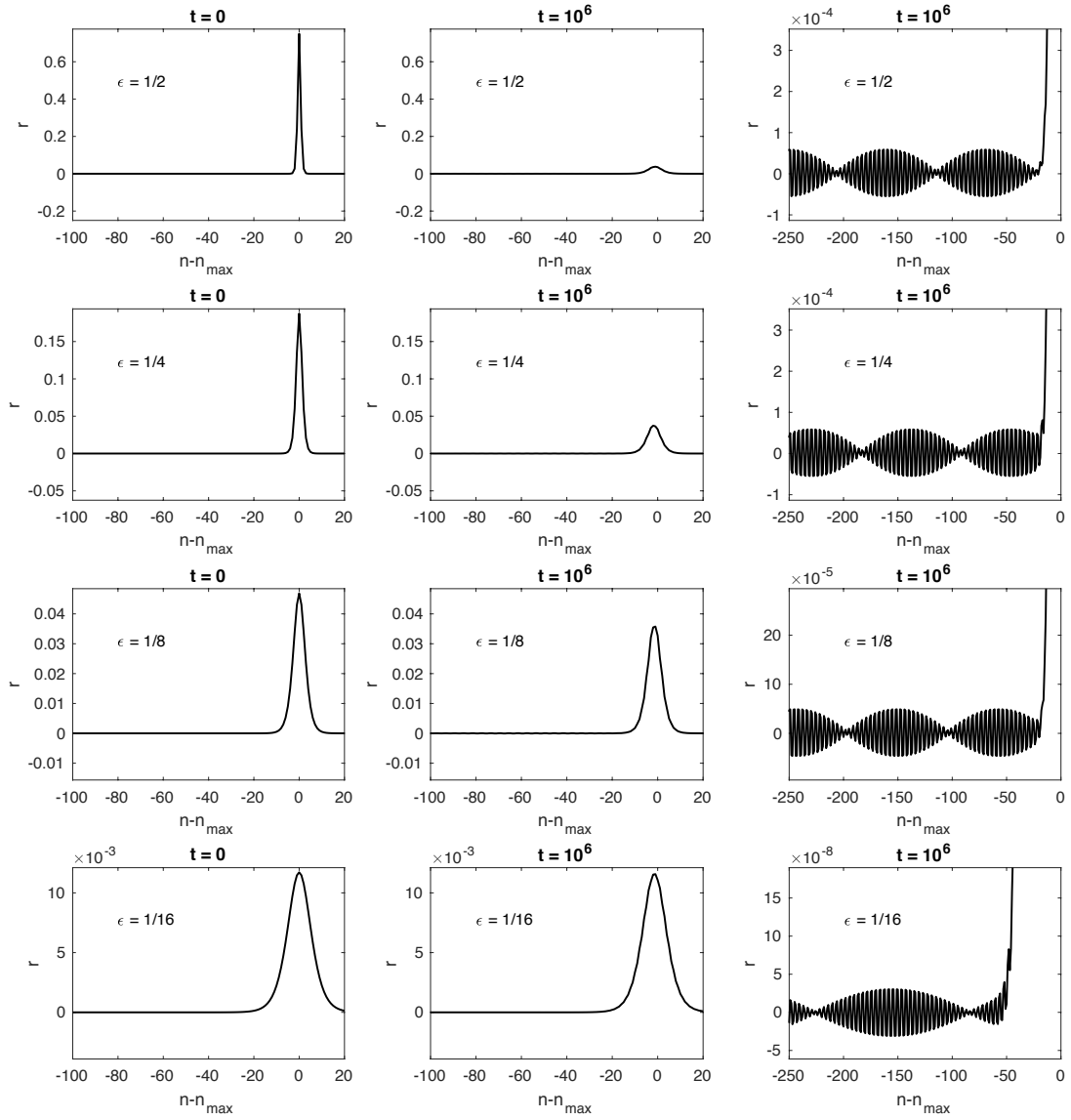

Figure 3. Plots of the $r-$component of the numerical computation of $\mathbf{\Psi}^{m_1,m_2,\varepsilon}(t)$ vs. n at $t = 0$ and $t = 10^6$. The final panel in each row is a close-up of the oscillatory wake immediately behind the main pulse at $t = 10^6$. In this figure, $m_1 = 1$ and $m_2 = \sqrt{2}$.

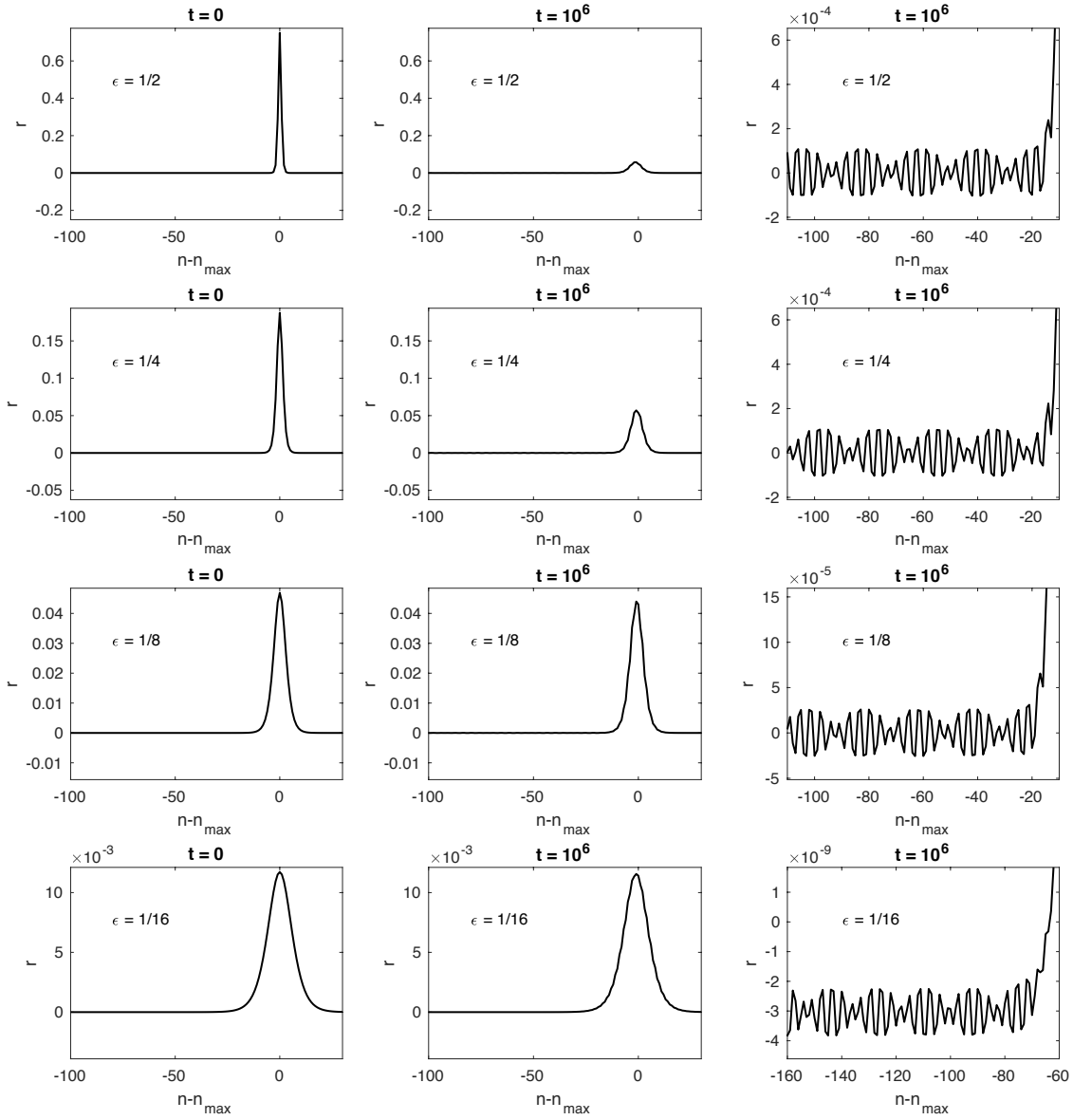

Figure 4. Plots of the $r-$component of the numerical computation of $\mathbf{\Psi}^{m_1,m_2,\varepsilon}(t)$ vs. n at $t = 0$ and $t = 10^6$. The final panel in each row is a close-up of the oscillatory wake immediately behind the main pulse at $t = 10^6$. In this figure, $m_1 = 1$ and $m_2 = 2$.

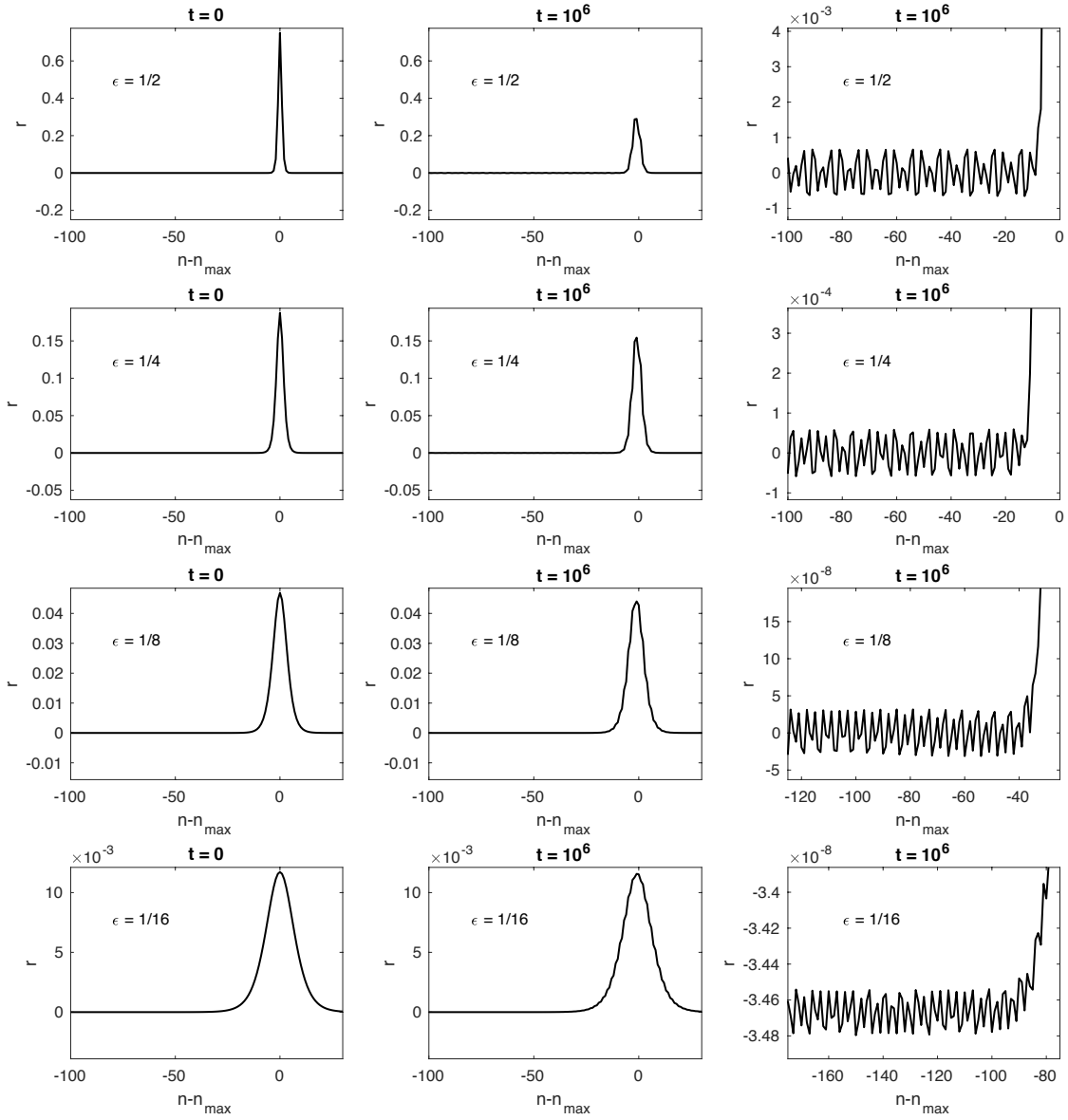

Figure 5. Plots of the $r-$component of the numerical computation of $\mathbf{\Psi}^{m_1,m_2,\varepsilon}(t)$ vs. n at $t = 0$ and $t = 10^6$. The final panel in each row is a close-up of the oscillatory wake immediately behind the main pulse at $t = 10^6$. In this figure, $m_1 = 1$ and $m_2 = \pi$.

3.2. Amplitudes vs. time

In Figures 6–8 we present plots of amp_{sol} and amp_{wake} vs. time for our runs. We present these on log – log plots. Here are our observations:

1. In each case, it is plain that there is an initial transient phase (corresponding to the initial

disordered wake) followed by a longer period where the dynamics are more regular.

2. In situations where ε is relatively large, the graphs follow a distinctly linear decay following the transient phase. Since the plots are log – log this indicates that these quantities are decaying at an algebraic rate.

3. When ε is smaller, the amp_{sol} and amp_{wake} settle into seemingly constant values.

4. Using a best fit approximation, we compute the rates of decay of amp_{sol} and amp_{wake} for those where the decay appears to algebraic. See Table 1. In this table, we denote the cases where the ultimate fate is seemingly constant by writing "~cst".

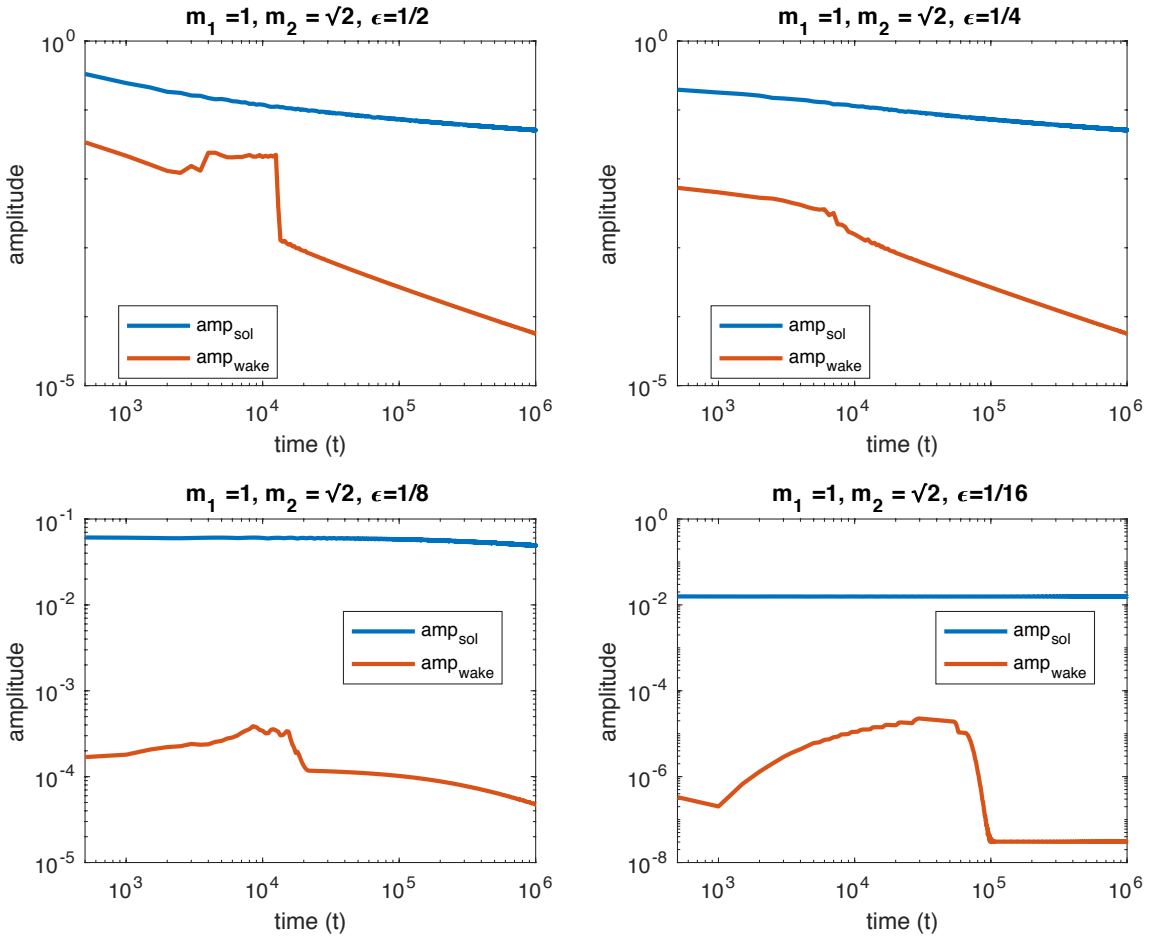

Figure 6. log – log plots of amplitudes of the leading solitary wave and oscillatory wakes vs. time when the mass ratio is $\sqrt{2}$.

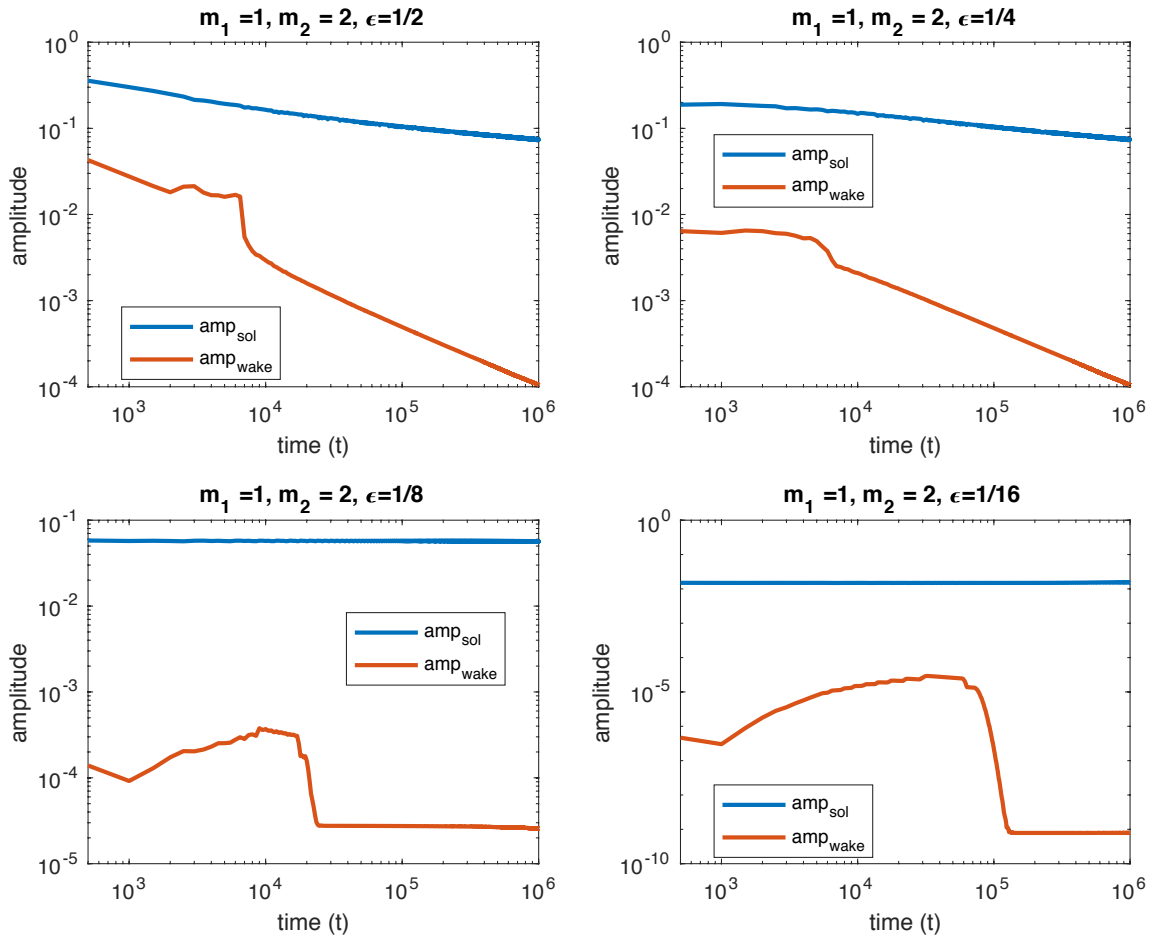

Figure 7. log – log plots of amplitudes of the leading solitary wave and oscillatory wakes vs. time when the mass ratio is 2.

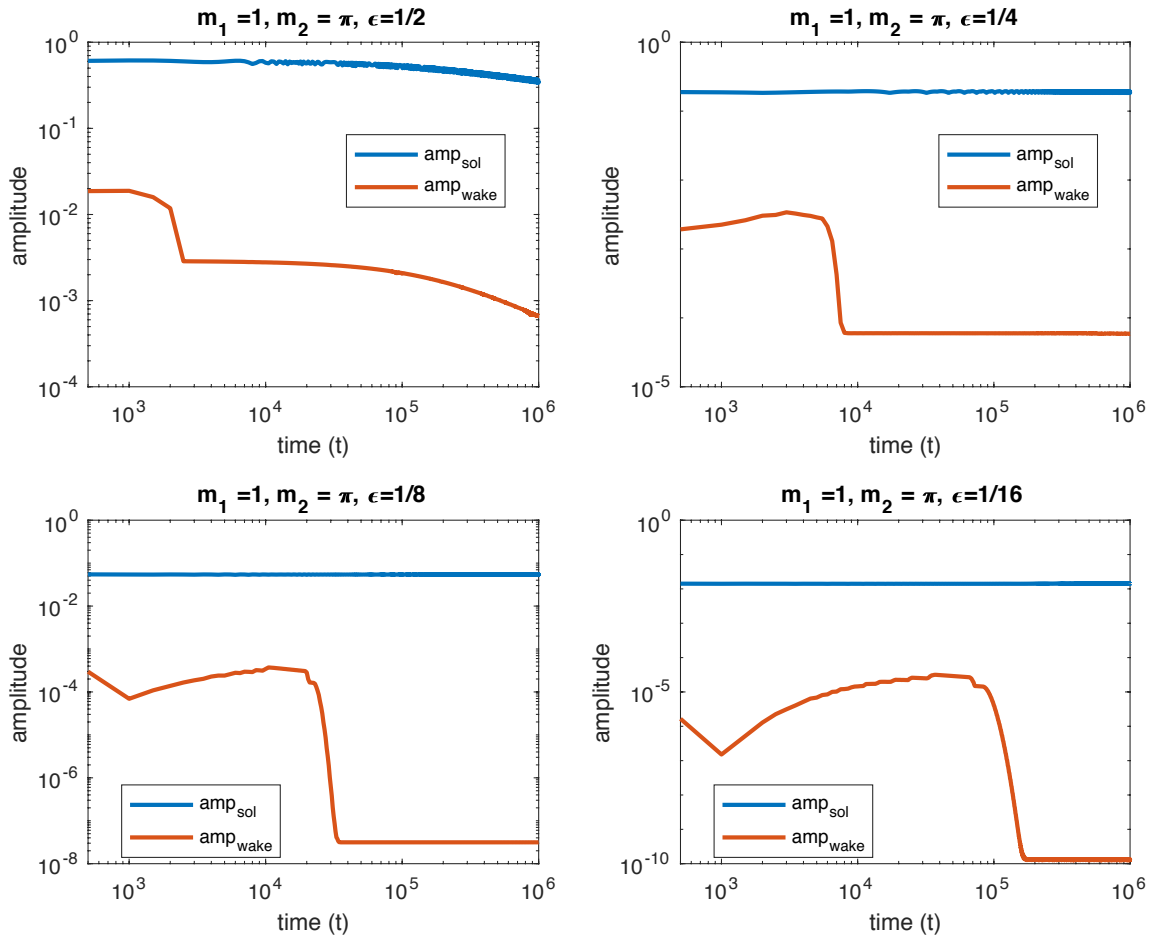

Figure 8. log – log plots of amplitudes of the leading solitary wave and oscillatory wakes vs. time when the mass ratio is π.

Table 1. Numerically computed rate of decay

mass ratio	ε	amp_{sol}	amp_{wake}
$\sqrt{2}$	$1/2$	$t^{-.1530}$	$t^{-.6710}$
$\sqrt{2}$	$1/4$	$t^{-.1524}$	$t^{-.6682}$
$\sqrt{2}$	$1/8$	$t^{-.0778}$	$t^{-.3591}$
$\sqrt{2}$	$1/16$	$\sim$cst	$\sim$cst
2	$1/2$	$t^{-.1457}$	$t^{-.6689}$
2	$1/4$	$t^{-.1425}$	$t^{-.6600}$
2	$1/8$	$\sim$cst	$\sim$cst
2	$1/16$	$\sim$cst	$\sim$cst
π	$1/2$	$t^{-.1778}$	$t^{-.5421}$
π	$1/4$	$\sim$cst	$\sim$cst
π	$1/8$	$\sim$cst	$\sim$cst
π	$1/16$	$\sim$cst	$\sim$cst

4. Conclusions

These simulations indicate that "solitary wave plus oscillatory wake" is the generic structure of $\mathbf{\Psi}^{m_1,m_2,\varepsilon}(t)$ when $t \gg 1$. This appears to be true over a range of mass ratios and values of ε. The general trend is that the amplitude of the wake is much smaller than that of the leading solitary wave but with a frequency seemingly fixed by the mass ratio. The likely cause of the oscillatory wake is a resonance between the acoustic and optical parts of the solution, though the precise mechanism is as yet unknown.

Since the problem conserves energy, it is impossible that both amp_{sol} and amp_{wake} are ultimately constant and nonzero, although some of our simulations seem to indicate that this is what is taking place. However, we conjecture that the rate of decay in these cases is actually so slow, slower even than algebraic, that it is undetectable using the methodology presented here. Given that the nanopterons from [1] and [11] have ripples which are small beyond all orders of ε, it seems within the realm of possibility that a truly rigorous treatment of the oscillatory wake will likewise involve a beyond all orders sort of analysis [19]. Such a treatment is beyond the scope of this investigation, but we feel our results demonstrate that such an analysis would be of great interest.

Acknowledgements

This work was supported by the National Science Foundation through grant DMS-1511488.

Conflict of interest

The authors declare no conflict of interest.

References

1. Faver TE, Wright JD (2018) Exact diatomic Fermi-Pasta-Ulam-Tsingou solitary waves with optical band ripples at infinity. *SIAM J Math Anal* 50: 182–250.
2. Lustri CJ, Porter MA (2018) Nanoptera in a period-2 Toda chain. *SIAM J Appl Dyn Syst* 17: 1182–1212.
3. Porter M, Daraio C, Szelengowicz I, et al. (2009) Highly nonlinear solitary waves in heterogeneous periodic granular media. *Phys D* 238: 666–676.
4. Gaison J, Moskow S, Wright JD, et al. (2014) Approximation of polyatomic FPU lattices by KdV equations. *Multiscale Model Simul* 12: 953–995.
5. Qin WX (2015) Wave propagation in diatomic lattices. *SIAM J Math Anal* 47: 477–497.
6. Betti M, Pelinovsky DE (2013) Periodic traveling waves in diatomic granular chains. *J Nonlinear Sci* 23: 689–730.
7. Chirilus-Bruckner M, Chong C, Prill O, et al. (2012) Rigorous description of macroscopic wave packets in infinite periodic chains of coupled oscillators by modulation equations. *Discrete Contin Dyn Syst Ser S* 5: 879–901. Available from: https://doi.org/10.3934/dcdss.2012.5.879.
8. Brillouin L (1953) *Wave Propagation in Periodic Structures. Electric Filters and Crystal Lattices*, 2Eds., New York: Dover Publications, Inc.
9. Tabata Y (1996) Stable solitary wave in diatomic Toda lattice. *J Phys Soc Jpn* 65: 3689–3691.
10. Okada Y, Watanabe S, Tanaca H (1990) Solitary wave in periodic nonlinear lattice. *J Phys Soc Jpn* 59: 2647–2658. Available from: https://doi.org/10.1143/JPSJ.59.2647.
11. Hoffman A, Wright JD (2017) Nanopteron solutions of diatomic Fermi-Pasta-Ulam-Tsingou lattices with small mass-ratio. *Phys D* 358: 33–59.
12. Vainchtein A, Starosvetsky Y, Wright JD, et al. (2016) Solitary waves in diatomic chains. *Phys Rev E* 93: 042210.
13. Schneider G, Wayne CE (1999) Counter-propagating waves on fluid surfaces and the continuum limit of the Fermi-Pasta-Ulam model, In: *International Conference on Differential Equations*, Vol. 1, 2 (Berlin, 1999), 390–404, World Sci. Publ., River Edge, NJ, 2000.
14. Friesecke G, Pego RL (1999) Solitary waves on FPU lattices: I. Qualitative properties, renormalization and continuum limit. *Nonlinearity* 12: 1601–1627.
15. Friesecke G, Pego RL (2002) Solitary waves on FPU lattices: II. Linear implies nonlinear stability. *Nonlinearity* 15: 1343–1359.
16. Friesecke G, Pego RL (2004) Solitary waves on Fermi-Pasta-Ulam lattices: III. Howland-type Floquet theory. *Nonlinearity* 17: 207–227.
17. Friesecke G, Pego RL (2004) Solitary waves on Fermi-Pasta-Ulam lattices: IV. Proof of stability at low energy. *Nonlinearity* 17: 229–251.

18. Mizumachi T (2009) Asymptotic stability of lattice solitons in the energy space. *Commun Math Phys* 288: 125–144.
19. Boyd JP (1998) *Weakly Nonlocal Solitary Waves and Beyond-All-Orders Asymptotics Generalized Solitons and Hyperasymptotic Perturbation Theory* , In Series: Mathematics and its Applications. Dordrecht: Kluwer Academic Publishers, vol. 442. Available from: https://doi.org/10.1007/978-1-4615-5825-5.
20. Faver T (2017) Nanopteron-stegoton traveling waves in spring dimer Fermi-Pasta-Ulam-Tsingou lattices, in press. Available from: https://arxiv.org/abs/1710.07376.
21. Lombardi E (2000) *Oscillatory Integrals and Phenomena Beyond All Algebraic Orders with Applications to Homoclinic Orbits in Reversible Systems*, In series: Lecture Notes in Mathematics. Berlin: Springer-Verlag, vol. 1741. Available from: https://doi.org/10.1007/BFb0104102.
22. Sun SM (1999) Non-existence of truly solitary waves in water with small surface tension. *Proc Math Phys Eng Sci* 455: 2191–2228.
23. Martínez AJ, Kevrekidis PG, Porter MA (2016) Superdiffusive transport and energy localization in disordered granular crystals. *Phys Rev E* 93: 022902. Available from: https://doi.org/10.1103/physreve.93.022902.
24. Hairer E, Lubich C, Wanner G (2006) *Geometric Numerical Integration: Structure-Preserving Algorithms for Ordinary Differential Equations*, 2Eds., In series: Springer Series in Computational Mathematics. Springer, Heidelberg, 2010, vol. 31.
25. Beyn WJ, Thümmler V (2004) Freezing solutions of equivariant evolution equations. *SIAM J Appl Dyn Syst* 3: 85–116.
26. Beyn WJ, Otten D, Rottmann-Matthes J (2018) Computation and stability of traveling waves in second order evolution equations. *SIAM J Numer Anal* 56: 1786–1817.
27. Beale JT (1991) Exact solitary water waves with capillary ripples at infinity. *Commun Pure Appl Math* 44: 211–257.
28. Sun SM (1991) Existence of a generalized solitary wave solution for water with positive Bond number less than 1/3. *J Math Anal Appl* 156: 471–504.
29. LeVeque RJ, Yong DH (2003) Solitary waves in layered nonlinear media. *SIAM J Appl Math* 63: 1539–1560.
30. LeVeque RJ, Yong DH (2003) Phase plane behavior of solitary waves in nonlinear layered media, In: *Hyperbolic Problems: Theory, Numerics, Applications*. Berlin: Springer, 43–51.
31. Kevrekidis PG, Stefanov AG, Xu H (2016) Traveling waves for the mass in mass model of granular chains. *Lett Math Phys* 106: 1067–1088.
32. Pnevmatikos S, Flytzanis N, Remoissenet M (1986) Soliton dynamics of nonlinear diatomic lattices. *Phys Rev B* 33: 2308–2321.

AIMS Press